ELSEVIER

Thermochimica Acta 354 (2000) 45–57

thermochimica acta

www.elsevier.com/locate/tca

Thermal decomposition of $[Co(NH_3)_6]_2(C_2O_4)_3{\cdot}4H_2O$ I. Identification of the solid products

Ewa Ingier-Stocka[a,*], Marek Maciejewski[b]

[a]*Institute of Inorganic Chemistry & Metallurgy of Rare Elements, Wroclaw University of Technology, Wybrzeze St. Wyspianskiego 27, PL 50-370 Wroclaw, Poland*

[b]*Laboratory of Technical Chemistry, Swiss Federal Institute of Technology, ETH-Zentrum, CH-8092 Zurich, Switzerland*

Received 26 July 1999; accepted 2 February 2000

Abstract

Investigation of the thermal decomposition of $[Co(NH_3)_6]_2(C_2O_4)_3{\cdot}4H_2O$ has been carried out in air and argon atmospheres under non-isothermal, isothermal and quasi-isothermal-isobaric conditions. Identification of intermediates and final products was carried out using spectroscopy (Far-IR, IR, UV–VIS), magnetic susceptibility and X-ray diffraction. The dissociation of the compound under investigation was found to occur in three stages in both atmospheres. The solid products formed at each particular stages of the decomposition has been identified.

Keywords: Thermal decomposition; $[Co(NH_3)_6]_2(C_2O_4)_3{\cdot}4H_2O$; XRD powder difractograms

1. Introduction

The present work is part of our studies to determine the mechanism of thermal decomposition of some amminecobalt complexes e.g. hexaaminecobalt(III) chloride and hexaamminecobalt(III) oxalate tetrahydrate [1–4]. These compounds seem to be interesting as intermediates for cobalt recovery [5]. It seems moreover that the latter compound may be a precursor for the low-temperature preparation of metallic cobalt, for example, in preparing catalysts. Numerous publications [6,7], are concerned with the thermal decomposition of transition metals oxalates but the literature referring to the thermal decomposition of $CoC_2O_4{\cdot}2H_2O$ disagree considerably in the temperature range of dehydration, the decomposition processes and the composition of the final products in an inert gas atmosphere, also much of the literature relating to the thermal decomposition of cobalt amminecomplexes is often contradictory or incomplete. A survey of the papers published up to 1966 has been made by Wendlandt and Smith [8], and are listed in Refs [1,9]. A fragment of Hadrich's dissertation [10] and an article by Jeyaraj and House [11] are devoted to the thermal decomposition of $[Co(NH_3)_6]_2(C_2O_4)_3{\cdot}4H_2O$. The results and conclusions published in these works are contradictory and some doubt is cast on their validity.

The aim of the work presented was to identify the intermediates and the final products of the thermal decomposition $[Co(NH_3)_6]_2(C_2O_4)_3{\cdot}4H_2O$ under non-isothermal, isothermal and quasi-isothermal-isobaric

* Corresponding author. Tel.: +48-71-328-43-30; fax: +48-71-328-43-30.
E-mail address: ingier@ichn.ch.pwr.wroc.pl (E. Ingier-Stocka)

0040-6031/00/$ – see front matter
PII: S0040-6031(00)00421-4

conditions in air and argon atmospheres and to propose the most probable sequences of thermal decomposition.

2. Experimental

2.1. Materials

2.1.1. Substrate

The compound $[Co(NH_3)_6]_2(C_2O_4)_3{\cdot}4H_2O$ was synthesized by the method described in [12]. The composition of the substrate was confirmed by elemental analysis and atomic absorption spectroscopy (AAS). The elemental analysis was: Co, 18.21% found, 17.93% calc.; H, 6.97% found, 6.73% calc.; C, 11.95% found, 10.94% calc.; N, 24.13% found, 25.53% calc.

2.1.2. Intermediates

Thermal decomposition of the substrate was carried out under different experimental conditions i.e. non-isothermal, isothermal and quasi-isothermal-isobaric in a known gas atmosphere up to set temperatures or for fixed periods of time. The solid products of the decomposition after cooling were submitted to further analysis.

The following symbols (in parentheses) are used throughout: substrate (S); intermediate (A′) at the end of the stage I ($-\Delta m \cong 11\%$) under non-isothermal or isothermal conditions; the intermediate (A) at the end of the stage I ($-\Delta m \cong 16\%$) under quasi-isothermal-isobaric conditions; the intermediate (B) at the end of the substage IIa ($-\Delta m \cong 51\%$) under non-isothermal and quasi-isothermal-isobaric conditions; the intermediate (C) at the end of the substage IIb ($-\Delta m \cong 55\%$) under non-isothermal, isothermal and quasi-isothermal-isobaric conditions; the intermediate (D) at the beginning of the stage III ($-\Delta m \cong 60\%$) under non-isothermal conditions; the intermediate (E) during the stage III ($-\Delta m \cong 70\%$) under non-isothermal conditions.

2.2. Apparatus and methods

Thermal analysis (TA) was carried out with a Derivatograph C (MOM, Budapest). The experiments were carried out under non-isothermal conditions with different heating rates (β) from 1 to 20°C min^{-1} in flowing ($\sim$4 dm^3 h^{-1}) air or argon of 99.99% purity using samples within the range 40 to 100 mg. Simultaneous TG-DTG-DTA curves were obtained in the range 20–500°C. Alumina crucibles were used both for the specimen and reference (α-Al_2O_3). Isothermal experiments were carried out as described in [4]. The quasi-isothermal-isobaric measurements were carried out under the following conditions: 20 to 600°C; weight 40 mg; heating rate 0.5 to 1.5°C min^{-1}; rate of mass loss 0.1–0.5 mg min^{-1}; flowing air or argon atmosphere ($\sim$4 dm^3 h^{-1}).

The TA measurements (TG, DTA) under non-isothermal conditions with heating rate 2.5, 5 and 10°C min^{-1} were carried out with a thermoanalyzer STA 409 (Netzch, Germany). The experiments were carried out in flowing argon or air using samples of a few tens of milligrams. Pt crucibles were used and the reference material was α-Al_2O_3. Diffuse reflectance spectra of the solids in Li_2CO_3 matrices were recorded in the range 800 to 200 nm with a Hitachi M 356 UV–VIS spectrophotometer.

X-ray diffraction patterns (XRD) were measured on a DRON-2 (USSR) and a Philips 1680 X Pert diffractometer using CuKα radiation.

Magnetic susceptibility was measured by Faradays' method within the range −193 to 20°C. The magnetic moment, μ_{eff}, values were calculated using the following expression:

$$\mu_{eff} = 2.83\sqrt{\chi_M(T-\Theta)} \quad (1)$$

where χ_M is the magnetic susceptibility, T the temperature in K and Θ the Weiss constant.

Infrared (IR) spectra were recorded on a SPECORD M 80/195 spectrometer between 4000–400 cm^{-1}. Spectra were measured on KBr discs. Far-IR spectra were recorded on a Perkin–Elmer M 180 spectrometer from 500–40 cm^{-1} using samples dispersed in Nujol.

3. Results

3.1. Thermal analysis

The thermal decomposition of $[Co(NH_3)_6]_2(C_2O_4)_3{\cdot}4H_2O$ in air and argon proceeded in three stages which was up to 500°C, see Fig. 1. The first stage was an endothermic process independent of

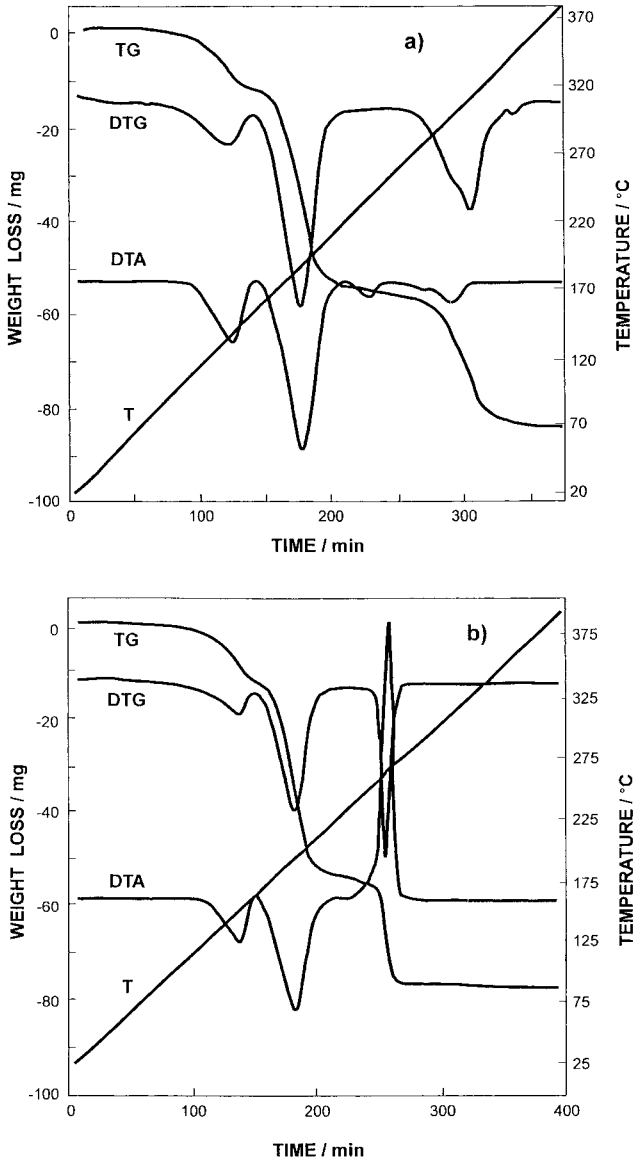

Fig. 1. TG-DTG-DTA curves for the decomposition of $[Co(NH_3)_6]_2(C_2O_4)_3{\cdot}4H_2O$; β=1°C min^{-1}; m=100 mg: (a) in argon, (b) in air.

the gas atmosphere. The second consisted of two substages, denoted as IIa and IIb, both were endothermic. The location of the end of the second stage was subjective and depended on the experimental conditions. It was arbitrarily assumed to corresponds with a mass loss of 55%. The third stage was also complex. In the inert gas atmosphere usually two endotherms were recorded (Table 1). These are the substages IIIa and IIIb — and they overlapped at low heating rates β<2°C min^{-1}, see Fig. 1a. However, in the air, see Fig. 1b, one large exotherm was seen. The TA results are summarised in Table 1. Temperature range and mass loss for the stages I and II in air and argon were close to each other while the third stage depended significantly on the atmosphere. In air, at the same heating rate and sample mass, the total decomposition

Table 1
Thermoanalytical results [TG-DTG-DTA] on $[Co(NH_3)_6]_2(C_2O_4)_3 \cdot 4H_2O$ decomposition in air and argon atmospheres

No.	Procedural parameters	Stage	Temperature range (°C)	DTA_p (°C)	Mass loss (%)		Residue
					Observed	Theoretical	
1[a]	78.72 mg TG	I	89–195	183_{endo}	10.8	10.9	$[Co(NH_3)_6]_2(C_2O_4)_3$
	73.80 mg DTA	IIa	195–275	231_{endo}	51.3	50.1	$CoC_2O_4 \cdot NH_3$
	β=5°C min^{-1}	IIb	275–305	287_{endo}	53.8	55.3	CoC_2O_4
	Argon	IIIa	305–360	338_{endo}	60.0	60.8	$CoO+CoC_2O_4$ (75 mol%)
		IIIb	360–410	385_{endo}	80.0	79.6	Co+CoO (50 mol%)
2[a]	78.54 mg TG	I	89–185	170_{endo}	11.1	10.9	$[Co(NH_3)_6]_2(C_2O_4)_3$
	73.80 mg DTA	IIa	185–260	218_{endo}	51.5	50.1	$CoC_2O_4 \cdot NH_3$
	β=2.5°C min^{-1}	IIb	260–285	270_{endo}	54.5	55.3	CoC_2O_4
	Argon	IIIa	285–345	330_{endo}	66.0	66.3	$CoO+CoC_2O_4$ (50 mol%)
		IIIb	345–390	359_{endo}	79.4	79.6	Co+CoO (50 mol%)
3[a]	78.56 mg TG	I	96–195	181_{endo}	10.9	10.9	$[Co(NH_3)_6]_2(C_2O_4)_3$
	58.72 mg DTA	II	196–270	230_{endo}	51.4	50.1	$CoC_2O_4 \cdot NH_3$
	β=5°C min^{-1}	III	270–345	309_{exo}	74.4	75.6	Co_3O_4
	Air						
4[a]	78.70 mg TG	I	80–180	168_{endo}	11.2	10.9	$[Co(NH_3)_6]_2(C_2O_4)_3$
	58.72 mg DTA	II	180–255	218_{endo}	52.1	52.8	$CoC_2O_4 \cdot 1/2NH_3$
	β=2.5°C min^{-1}	III	255–330	294_{exo}	74.5	75.6	Co_3O_4
	Air						
5[b]	TG-DTG-DTA	I	105–206	190_{endo}	11.0	10.9	$[Co(NH_3)_6]_2(C_2O_4)_3$
	100.0 mg	IIa	206–285	234_{endo}	50.9	50.1	$CoC_2O_4 \cdot NH_3$
	β=5°C min^{-1}	IIb	285–320	301_{endo}	53.5	55.3	CoC_2O_4
	Argon	IIIa	320–365	349_{endo}	60.8	60.8	$CoO+CoC_2O_4$ (75 mol%)
		IIIb	365–426	396_{endo}	80.1	79.6	Co+CoO (50 mol%)
6[b]	TG-DTG-DTA	I	98–163	136_{endo}	12.1	10.9	$[Co(NH_3)_6]_2(C_2O_4)_3$
	41.2 mg	II	163–283	200_{endo}	55.5	55.3	CoC_2O_4
	β=1°C min^{-1}	III	283–383	321_{endo}	83.7	82.1	Co
	Argon						
7[b]	TG-DTG-DTA	I	101–171	149_{endo}	11.9	10.9	$[Co(NH_3)_6]_2(C_2O_4)_3$
	100.9 mg	II	171–284	205_{endo} 261_{endo}	55.7	55.3	CoC_2O_4
	β=1°C min^{-1}	III	284–386	324_{endo}	83.1	82.1	Co
	Argon						
8[b]	TG-DTG-DTA	I	92–158	138_{endo}	11.4	10.9	$[Co(NH_3)_6]_2(C_2O_4)_3$
	40.6 mg	II	158–260	197_{endo}	55.0	55.3	CoC_2O_4
	β=1°C min^{-1}	III	260–279	274_{exo}	75.7	75.6	Co_3O_4
	Air						
9[b]	TG-DTG-DTA	I	99–170	158_{endo}	11.8	10.9	$[Co(NH_3)_6]_2(C_2O_4)_3$
	100.4 mg	II	170–272	202_{endo}	54.6	55.3	CoC_2O_4
	β=1°C min^{-1}	III	272–285	282_{exo}	75.9	75.6	Co_3O_4
	Air						

[a] The measurements No. 1–4 were done on a Netzch STA 409 (Germany) apparatus.
[b] The measurements No. 5–9 were done on a Derivatograph C (MOM Budapest) apparatus.

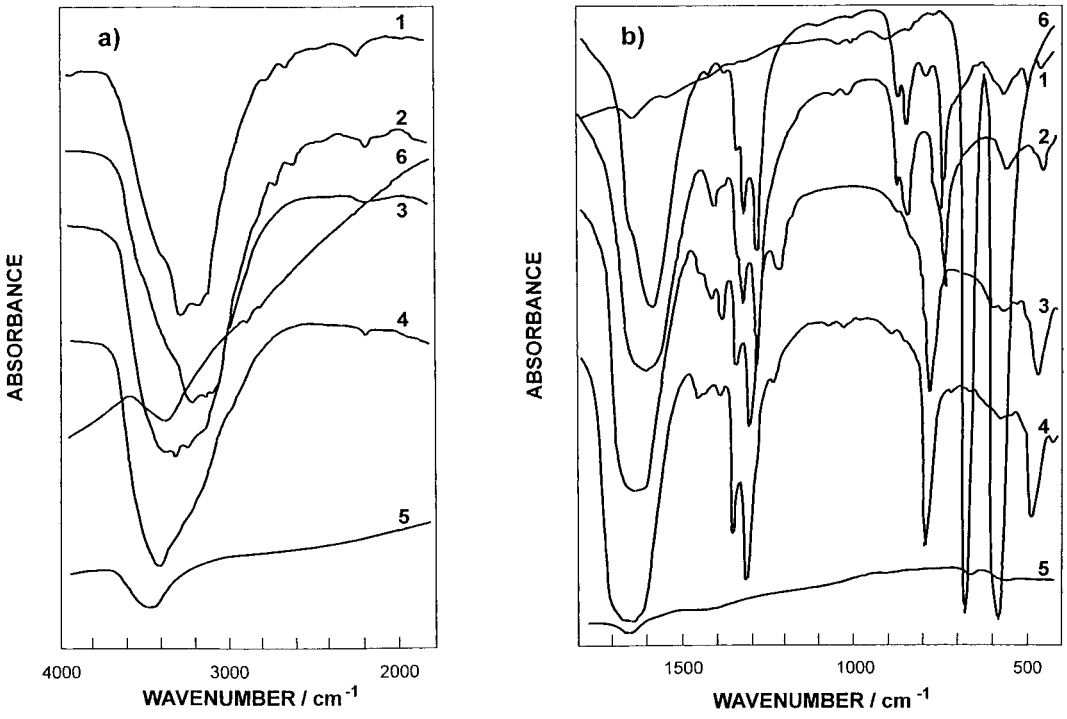

Fig. 2. IR spectra of $[Co(NH_3)_6]_2(C_2O_4)_3{\cdot}4H_2O$ and the intermediates of its decomposition: 1, the substrate; 2, the intermediate A both in air and argon ($-\Delta m$=16%); 3, the intermediate B both in air and argon ($-\Delta m$=51%); 4, the intermediate C both in air and argon ($-\Delta m$=55%); 5, the final product in argon; 6, the final product in air.

ended at a lower temperature than in argon. The observed mass loss was also lower and this pointed to some difference in the final decomposition products in argon and air.

3.2. Spectroscopic studies

3.2.1. IR and far IR spectroscopy

The IR and Far IR spectra of the substrate, the intermediates and the final products of degradation in air and argon atmospheres are showed in Figs. 2 and 3. The spectra of the intermediates during decomposition in air and argon were identical, independent of experimental conditions (non-isothermal, isothermal or quasi-isothermal-isobaric). Analysis was carried out on the basis of literature assignments [13–25].

The spectrum of the substrate, see Fig. 2 curve 1, exhibited a series groups of bands, some of which were typical of hexaamminecobalt(III) complexes [13,14]. In spectrum No. 1, see Fig. 2, a strong complex absorption band is seen in the range 3400–3100 cm^{-1} which can be assigned to the stretching vibrations of the NH_3 ($\nu_{a(NH)}$=3290 cm^{-1} and $\nu_{s(NH)}$=3180 cm^{-1}; 3120 cm^{-1}) and to H_2O groups ($\nu_{s(OH)}$ and $\nu_{a(OH)}\sim$3300 cm^{-1}). An intensive band at $\sim$1600 cm^{-1} is due to the bending vibrations of NH_3 ($\delta_{a(HNH)}$), crystallization water ($\delta_{a(HOH)}$ $\sim$1660 cm^{-1}) and/or some stretching vibrations $C_2O_4^{2-}$ ions ($\nu_{a(CO)}$). The series of bands in the range 1450–1300 cm^{-1} as well as the shoulder at $\sim$1365 cm^{-1} probably originate from the symmetrical bending mode of the NH_3 groups ($\delta_{s(HNH)}$=1343 cm^{-1}) and from the stretching of the $C_2O_4^{2-}$ ion ($\nu_{s(CO)}$=1305 cm^{-1}). In the range 900–650 cm^{-1} a strong band at 876 cm^{-1} and a weaker one 820 cm^{-1} originated from rocking vibrations of NH_3, $\rho_{r(NH_3)}$.The wagging vibrations in H_2O molecule can also take part in the last band. The weak band at 900 cm^{-1} and the strong one 770 cm^{-1} can be assigned to stretching ($\nu_{s(CO)}$) and bending ($\delta_{a(OCO)}$) vibrations in an oxalate ion. Between 650 and 400 cm^{-1} (Fig. 2b and Fig. 3) there are three weak

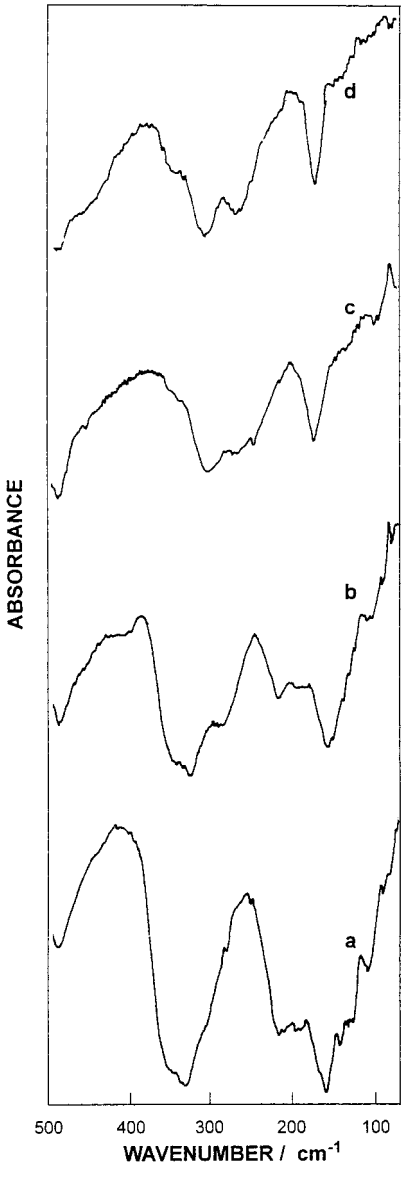

Fig. 3. FIR spectra of $[Co(NH_3)_6]_2(C_2O_4)_3{\cdot}4H_2O$ and the intermediates of its decomposition in air: (a) the substrate; (b) the intermediate A ($-\Delta m$=16%); (c) the intermediate B ($-\Delta m$=51%); (d) the intermediate C ($-\Delta m$=55%).

bands resulting successively from: stretching vibrations of the Co(III)–N bond or bending vibrations in $C_2O_4^{2-}$ ion ($\delta_{s(CCO)}$ or $\delta_{(OCO)}$) — the band at $\sim$490 cm^{-1}, stretching vibrations in $C_2O_4^{2-}$ ($\nu_{(CC)}$) and/or oscillations in a molecule of crystallization water — the bands at 598 and 525 cm^{-1}. Below 400 cm^{-1} the strong band at 332 cm^{-1} is assigned to the bending vibrations $\delta_{(NCoN)}$ of the Co(III)–N bond. The shoulders at $\sim$345 and $\sim$218 cm^{-1} can originate from stretching and bending vibrations ($\nu_{(CC)}+\delta_{(OCO)}$), respectively, as well as from $\rho_{r(CO_2)}$ in an oxalate ion. According to the data of Dik et al. [15] the location of the band resulting from wagging vibrations, ρ_w, in a $C_2O_4^{2-}$ ion at $\sim$340 cm^{-1} suggests a distortion of the planar structure of a free oxalate ion (D_{2h} symmetry) resulting from the presence of hydrogen bonds in the structure of the crystal. Bands below 200 cm^{-1} include some lattice vibrations. The position of majority of bands originated from $C_2O_4^{2-}$ group vibrations observed in IR spectrum of the substrate is the closest to those given by Nakamoto [13] for a free oxalate ion (D_{2h} symmetry) or this one in $(NH_4)_2C_2O_4{\cdot}H_2O$ [15]. Their presence is due to the ionic bonding of the oxalate group with the complex cation in the substrate and also due to a possible participation of hydrogen bridges. Summing up the above, one can state that the bands characteristic for the complex cation $[Co(NH_3)_6]^{3+}$ vibrations are overlapped by the bands resulting from vibrations in a $C_2O_4^{2-}$ ion as well as in a H_2O molecule.

As it is seen in Figs. 2 and 3, the IR and FIR spectra of consecutive intermediates change gradually in comparison with the substrate spectrum; there are small changes in the range 4000–1500 cm^{-1} with slight shifts in the maxima to higher frequencies.

In the spectrum of intermediate A, see Fig. 2 curve 2, the bands resulting from the vibrations of crystallization water located at $\sim$1660 cm^{-1} (a shoulder), 820 and 525 cm^{-1} disappears, consistent with the dehydration of the substrate during stage I. This is consistent with the TA results. Important changes are observed in the spectrum in the range 1450–1200 cm^{-1} (Fig. 2b) characteristic of oxalate group bound to different compounds. The appearance of a new band at 1435 cm^{-1} and a shoulder at $\sim$1405 cm^{-1} suggests that the oxalate ion is bound to the inner coordination sphere of the metal. The changes to the FIR spectrum of intermediate A (Fig. 3, curve b) described below confirms this. At $\sim$415 cm^{-1} a shoulder appears which results from Co(III)–O stretching vibrations. The shoulder at about 290 cm^{-1} is assigned to oscillations of a metal–ligand bond in the complex cations $[Co(NH_3)_5X]^{n+}$ (C_{4v} symmetry) and trans-$[Co(NH_3)_4X_2]^{n+}$ (D_{4h} symme-

try) and/or the N–Co–X and/or N–Co–N bending vibrations in the complex cations mentioned above [13,16,17].

The IR spectrum of intermediate B (Fig. 2, curve 3) differs considerably from that of the substrate and intermediate A (Fig. 2, curves 1 and 2) below 1500 cm^{-1}. At ~1465 cm^{-1} a shoulder appears while a clear band with a maximum at 1400 cm^{-1} forms from the shoulder at ~1405 cm^{-1}, see curve 2 Fig. 2b. This suggests consecutive changes in the mode of $C_2O_4^{2-}$ ion bonding in the compound. Moreover, the band at 1342 cm^{-1} present in curves 1 and 2 of Fig. 2b and assigned to $\delta_{s(HNH)}$ disappears and a band at 1238 cm^{-1} appears. The latter is not present in the spectrum of intermediate C (curve 4, Fig. 2b) what suggests that it is the band $\delta_{s(HNH)}$ shifted from 1342 cm^{-1}. The sequence of bands in IR spectrum of product B i.e.: 1625_s, 1465_{sh}, 1435_w, 1400_w, 1358_m, and 1318_s cm^{-1} points to the $C_2O_4^{2-}$ acting in the product B as a bi- and quadridentate ligand [13,18–22]. It should be mentioned that the presence of ammonium oxalate cannot be excluded from intermediate A and B when comparing quantity and position of the bands in the region 3500–1200 cm^{-1} with the standard $(NH_4)_2C_2O_4 \cdot H_2O$ [23,24]. The band at 487 cm^{-1} observed earlier (Fig. 2, curves 1 and 2) and assigned to the $\delta_{(OCO)}$ and/or $\delta_{(CCO)}$ vibrations in $C_2O_4^{2-}$ becomes more intensive in B. The decrease in the band intensity at 332 cm^{-1} (see curve c in Fig. 3) assigned to the bending vibrations of the N–Co(III)–N bond suggests some loss of NH_3. The split band at 303–278 cm^{-1} attributed to the bending vibrations of the O–Co(II)–O bond in $CoC_2O_4 \cdot 2H_2O$ [10] may suggest reduction of Co(III) to Co(II). Moreover, the component of the mentioned band with maximum at 278 cm^{-1} probably originates from the wagging vibrations of the oxalate ion with a planar conformation. This suggests that the hydrogen bridges present in the substrate and the product A disappear. The clear band at 197 cm^{-1} present in the substrate and the product A is shifted to 176 cm^{-1}. In this region the N–Co(II)–N bending vibrations appear [13,16,25].

The IR and FIR spectra of the intermediate C are very similar to those of the synthesized $CoC_2O_4 \cdot 2H_2O$ and the product of its dehydration [10,26]. The band located at 3385 cm^{-1} may be assigned to the presence of some water adsorbed on the product between the measurements TA and IR. The location and the number of bands within the range 1800–1200 cm^{-1} originated from the oxalate group vibrations do not change in comparison with the product B which means that $C_2O_4^{2-}$ ion acts as a bi- and a quadridentate ligand also in the product C. The band at 1238 cm^{-1} ($\delta_{s(HNH)}$) almost disappeared. Comparing the FIR spectra of the substrate and the intermediates A–C (curves a–d, Fig. 3) within the region characteristic for lattice vibrations (250–40 cm^{-1}) it may be stated that the structures of the substrate and the product A are very similar. They change only in the products B and C what is connected with significant change of the substrate lattice.

As already mentioned the IR and FIR spectra of the corresponding decomposition intermediates of the compound under investigation in argon and air were identical, whereas the spectra of the final products differ significantly. The curve 5 (Fig. 2) — the final product of the decomposition in argon — exhibits only three residual bands i.e. at ~3360 cm^{-1}, resulting from the adsorbed water, as well as at 650 and 550 cm^{-1} characteristic for CoO [14]. A slight intensity of the last ones evidences that CoO is in the final product in a trace quantity only. In the spectrum of the final product obtained in the air there are two visible very strong and sharp bands at 662 and 561 cm^{-1} characteristic for Co_3O_4 [14].

Summing up these results for the IR and FIR spectroscopic studies of the $[Co(NH_3)_6]_2(C_2O_4)_3 \cdot 4H_2O$ thermal decomposition we conclude that

- dehydration of the compound under investigation occurs at the first stage of the decomposition (disappearance of the bands originated from H_2O molecule vibrations);
- the oxalate group, ionically bound to the substrate, enters into the inner coordination sphere of the complex as a mono- and/or bidentate ligand;
- the $C_2O_4^{2-}$ ion conformation changes from a distorted planar one in the substrate to a planar one in the intermediates B and C;
- at the second stage of the decomposition the reduction of Co(III) to Co(II) occurs and cobalt(II) oxalate is the product of stage II of the dissociation (intermediate C) with the $C_2O_4^{2-}$ group bounded as a bi- and quadridentate ligand;
- in the final product of the decomposition in argon there are trace quantities of CoO;

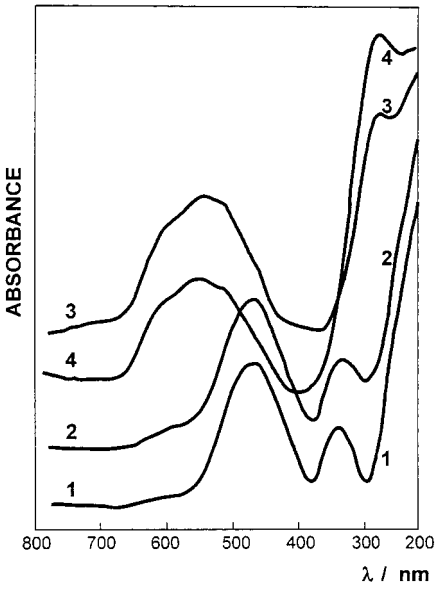

Fig. 4. Diffuse reflectance spectra of $[Co(NH_3)_6]_2(C_2O_4)_3{\cdot}4H_2O$ and the intermediates of its decomposition in argon: 1, the substrate; 2, the intermediate A′ ($-\Delta m$=11%); 3, the intermediate B ($-\Delta m$=51%); 4, the intermediate C ($-\Delta m$=55%).

- the final product of the decomposition in air is Co_3O_4.

3.2.2. UV–VIS spectroscopy

The diffuse reflectance spectra of substrate and intermediates A′, B and C are presented in Fig. 4. The spectra of the corresponding intermediates in the decomposition in air and argon atmospheres were found to be identical. The TA conditions did not change the intermediates spectra. The spectra of the substrate and intermediate A′ are very similar (see spectra No.1 and 2). These contained two bands at 472 (S) or 476 (A′) and 340 nm (S and A′) as well as a weak shoulder at ~590 nm (S and A′). Such spectra are characteristic of low-spin octahedral cobalt(III) compounds [27]. The spin-allowed transitions $^1A_{1g} \rightarrow {}^1T_{1g}$ (476 nm), $^1A_{1g} \rightarrow {}^1T_{2g}$ (340 nm) and additionally the spin-forbidden transition $^1A_{1g} \rightarrow {}^3T_{2g}$ in the complex ion $[Co(NH_3)_6]^{3+}$ were established to be responsible for the observed bands in the substrate and the intermediate A′ [27,28]. The spectra obtained for the substrate and the intermediate A′ are in agreement with those presented by Hadrich [10] for $[Co(NH_3)_6]_2(C_2O_4)_3{\cdot}4H_2O$ and $[Co(NH_3)_6]_2(C_2O_4)_3$, respectively.

In comparison with the substrate, some clear changes are shown in the spectra of the intermediates B and C being similar to each other. The presence of two bands i.e. a broad complex band with maximum at 545 (B) and 555 nm (C) as well as a narrow single band at 280 nm is characteristic of these intermediates. The band at 280 nm is characteristic for electronic transitions type charge-transfer (CT) in Co(II) compounds [27]. The spectrum of the intermediate B is similar to the spectra presented in literature [18,29] for Co(II) compounds with an octahedral structure (O_h) or a pseudo-octahedral one i.e. $K_2[Co(C_2O_4)_2]$ and $K_2[Co(C_2O_4)_2]{\cdot}6H_2O$ as well as $Co[Co(C_2O_4)_2]{\cdot}4H_2O$. These facts combined with the elemental analysis results allow to suggest that the intermediate B is the compound with the tetragonal symmetry with the formula $Co[Co(NH_3)_2(C_2O_4)_2]$ (octahedrically coordinated ions $[Co(NH_3)_2(C_2O_4)_2]^{2-}$ and Co^{2+} as counter-ions) or the compound with the formula $Co[Co(C_2O_4)_2]{\cdot}2NH_3$. The observed shift of the d–d band from 476 to ~550 nm suggests the formation of some pseudooctahedral high-spin (d^7) cobalt(II) compounds during the second stage. The spectrum of the intermediate C is the most similar to the spectra of CoC_2O_4 [19,26] and $[Co(NH_3)_4]^{2+}$ [27] (the first with the tetragonal symmetry, the second — tetrahedral) as well as to the square-planar cobalt(II) compounds [30] and binuclear cobalt(II) complex compounds [31]. In relation to the above described ambiguity, the spectrum of the intermediate C solution in dioxane was made. It exhibited two bands: a strong one with maximum at 508 nm and a shoulder at 476 nm and a weak, broad in the range 662–608 nm with maximum at 636 nm. It suggests that the intermediate C is the Co^{2+} ion surrounded by six oxygen atoms.

3.3. Magnetic susceptibility

Magnetic susceptibility of the substrate and the intermediates A and B have been measured. The calculated magnetic moment values, μ_{eff} are listed in Table 2 together with literature values μ_{eff} for some selected Co(II) compounds. The substrate was diamagnetic as expected for literature studies, e.g. for Co(III) ion in octahedral coordination, configuration d^6, spin-paired [32]. The intermediate A appears to be slightly paramagnetic. Assuming the formula

Table 2
Magnetic moments of the intermediates of $[Co(NH_3)_6]_2(C_2O_4)_3{\cdot}4H_2O$ thermal decomposition and, for comparison, of some cobalt(II) compounds

Compound	Temperature (K)	μ_{eff} (B.M.)	Ref.
$[Co(NH_3)_6]_2(C_2O_4)_3{\cdot}4H_2O$	80–293	~0 (diamagnetic)	This work
Intermediate A ($-\Delta m$=16%)	293	~0.85 (slightly paramagnetic)	This work
Intermediate B ($-\Delta m$=51%)			
$CoC_2O_4{\cdot}NH_3$	293	4.19	This work
$CoC_2O_4{\cdot}NH_3{\cdot}1/2H_2O$	293	4.32	This work
CoC_2O_4	300–420	4.97	[33]
$CoCO_3$	300–350	4.34	[33]
$K_2[Co(C_2O_4)_2]$	80–296	5.0	[33]
α-$CoC_2O_4{\cdot}0.3H_2O$	293	4.61	[10]
β-$CoC_2O_4{\cdot}0.1H_2O$	293	4.66	[10]
$4CoC_2O_4{\cdot}5NH_3$	293	4.49	[10]
$4CoC_2O_4{\cdot}3NH_3{\cdot}H_2O$	293	5.05	[10]

$[Co(NH_3)_5C_2O_4]_2C_2O_4$ corresponding to $-\Delta m$=16%, the magnetic moment value was 0.85 B.M. (Bohr Magneton). This suggests that at the beginning of stage II of the decomposition (T~470 K) the reduction of Co(III) to Co(II) has started, and this is in agreement with [8] on $[Co(NH_3)_6]Cl_3$ decomposition. The magnetic moment values of 4.32 and 4.19 B.M. for intermediate B were calculated assuming a formulae of $CoC_2O_4{\cdot}NH_3{\cdot}1/2H_2O$ or $CoC_2O_4{\cdot}NH_3$ (see Table 2) based on the elemental analysis results. The values lie within the range 4.1–5.2 B.M. characteristic of high-spin d^7 Co(II) compounds with the tetrahedral (T_d) or octahedral (O_h) structure [32]. The observed magnetic moment value 4.32 B.M. was nearest to 4.34 B.M. determined for $CoCO_3$ [33] and 4.49 B.M. measured by Hadrich [10] for a compound with the stoichiometric formula $4CoC_2O_4{\cdot}5NH_3$ (Table 2).

According to the literature [32,34,35] μ_{eff} values within the range 4.1–4.7 B.M. are characteristic of high-spin Co(II) compounds with tetrahedral structures. They are also observed in binuclear Co(II) compounds with a pseudo-octahedral structure [31,35] or polymeric Co(II) compounds with octahedral structures [36]. The magnetic moment values are consistent with the reduction of Co(III) to Co(II) during the second stage.

3.4. XRD analysis

X-ray powder diffraction analysis was used to investigate intermediates and the final products of the thermal decomposition of the substrate under non-isothermal, isothermal and quasi-isothermal-isobaric conditions in the air and argon atmospheres. Unmistakably they identified the final products as Co_3O_4 (air) or a mixture of CoO and Co with different quantitative composition or Co only (argon) (see Table 3) depending on the decomposition conditions. The JCPDS data base was used to analyse the diffractograms [37]. The intermediates at the second and

Table 3
Final products of the thermal decomposition of $[Co(NH_3)_6]_2(C_2O_4)_3{\cdot}4H_2O$ at different experimental conditions identified by XRD

Lp.	Final product	Atmosphere	Heating method
1	Co_3O_4	Air	Non-isothermal
2	Co_3O_4	Air	Isothermal
3	CoO+Co	Air	Quasi-isothermal-isobaric
4	CoO+Co	Argon	Isothermal
5	CoO+Co	Argon or nitrogen	Non-isothermal
6	Co	Argon or nitrogen	Quasi-isothermal-isobaric
7	Co	Argon	Non-isothermal

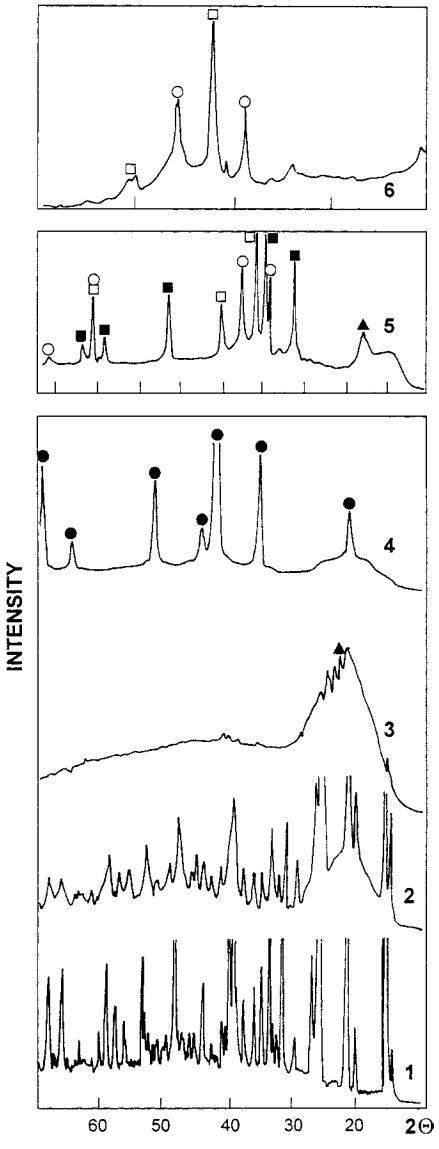

Fig. 5. XRD powder diffractograms of $[Co(NH_3)_6]_2(C_2O_4)_3{\cdot}4H_2O$ as well as the intermediates and the final products of its decomposition in air and argon: 1, the substrate; 2, the intermediate A′ ($-\Delta m$=11%); 3, the intermediate C ($-\Delta m$=55%); 4, the final product in air; 5, the final product in argon (non-isothermal conditions, β=5°C min^{-1}); 6, the final product in argon (quasi-isothermal-isobaric conditions) (▲) CoC_2O_4; (●) Co_3O_4; (■) CoO; (○) α-Co; (□) β-Co.

third stage of the decomposition were amorphous or very poorly crystallized, see Figs. 5 and 6. The powder diffractograms of the intermediates after stage I and II were identical, independently of the atmosphere. The diffractogram of the intermediate A′ (Fig. 5, curve 2) did not show any differences for that of the substrate, see Fig. 5 curve 1. The diffractogram of the sample D, see Fig. 6 curve b, showed reflections due to final product i.e. Co_3O_4 (JCPDS 09-0418) although they are present together with those characteristic of CoC_2O_4 (JCPDS 37-0719). The diffraction lines characteristic of Co_3O_4 are observed in the diffraction pattern of the intermediate E (Fig. 6, curve c) and the end-product obtained in the air atmosphere ($-\Delta m$=75.5%; Fig. 5, curve 4). The X-ray patterns of the final products of the decomposition in the argon atmosphere (Fig. 5, curve 6) indicate the presence of both forms of cobalt i.e. low-temperature α-Co (JCPDS 05-0727) and high-temperature β-Co (JCPDS 15-0806).

4. Conclusions

On the basis of mass losses on heating and analysis investigation of the solid intermediates and final products, as well as taking into account literature studies on the thermal decomposition of amminecobalt complexes e.g. [8,38] the following sequences of the thermal decomposition of $[Co(NH_3)_6]_2(C_2O_4)_3{\cdot}4H_2O$ are proposed:

Stage I (air, argon)

Non-isothermal and isothermal conditions

$$[Co(NH_3)_6]_2(C_2O_4)_3 \cdot 4H_2O \overset{endo}{\rightarrow} [Co(NH_3)_6]_2(C_2O_4)_3 + 4H_2O \quad (2)$$

Quasi-isothermal-isobaric conditions

$$[Co(NH_3)_6]_2(C_2O_4)_3 \cdot 4H_2O \rightarrow [Co(NH_3)_{6-n}C_2O_4]_2(C_2O_4) + 2nNH_3 + 4H_2O \quad (3)$$

where n=1 or 2

Stage II (air, argon)

Non-isothermal and isothermal conditions

$$3[Co(NH_3)_6]_2(C_2O_4)_3 \overset{endo}{\rightarrow} 3Co[Co(C_2O_4)_2] + N_2 + 34NH_3 + 3H_2O + 3CO + 3CO_2 \quad (4)$$

$$3CO + \tfrac{3}{2}O_2 \overset{exo}{\rightarrow} 3CO_2 \ \text{(secondary reaction in air)} \quad (5)$$

Quasi-isothermal-isobaric conditions

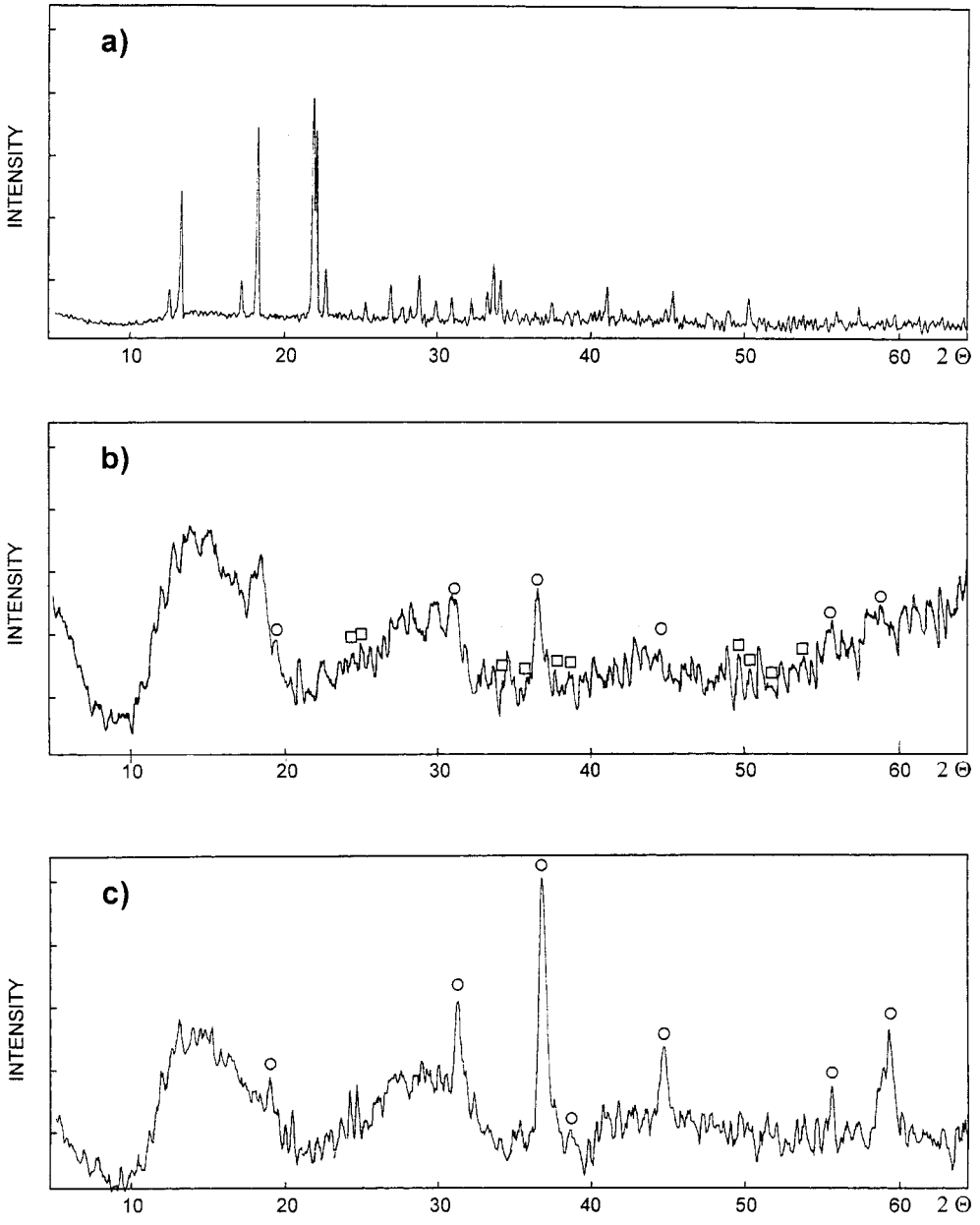

Fig. 6. XRD powder diffractograms of $[Co(NH_3)_6]_2(C_2O_4)_3{\cdot}4H_2O$ as well as the intermediates and the final products of its decomposition in air in non-isothermal conditions: (a) the substrate; (b) the intermediate D ($-\Delta m$=60%); (c) the intermediate E ($-\Delta m$=70%); (□) CoC_2O_4; (○) Co_3O_4.

$$3[Co(NH_3)_{6-n}C_2O_4]_2(C_2O_4) \rightarrow 3Co[Co(C_2O_4)_2] + N_2 + (34\text{-}6n)NH_3 + 3H_2O + 3CO + 3CO_2 \quad (6)x$$

Stage III (air)
Non-isothermal and isothermal conditions

$$3Co[Co(C_2O_4)_2] + 4O_2 \xrightarrow{exo} 2Co_3O_4 + 12CO_2 \quad (7)$$

or

$$3Co[Co(C_2O_4)_2] \xrightarrow{exo} 2Co_3O_4 + 8CO + 4CO_2 \quad (7a)$$

$$8CO + 4O_2 \xrightarrow{exo} 8CO_2 \quad \text{(secondary reaction in air)} \quad (7b)$$

Quasi-isothermal-isobaric conditions

$$Co[Co(C_2O_4)_2] \rightarrow Co + CoO + 3CO_2 + CO \quad (8)$$

Stage III (argon)

Non-isothermal, isothermal conditions

$$Co[Co(C_2O_4)_2] \xrightarrow{endo} 2Co + 4CO_2 \quad (9)$$

$$Co[Co(C_2O_4)_2] \xrightarrow{endo} 2CoO + 2CO + 2CO_2 \quad (10)$$

Quasi-isothermal-isobaric conditions reaction (9) only

The first stage in the decomposition is dehydration, followed by decomposition of the anhydrous salt and reduction of Co(III) to Co(II) in the second stage. The third stage in air is decomposition of $Co[Co(C_2O_4)_2]$ to Co_3O_4 and in argon, $Co[Co(C_2O_4)_2]$ decomposes to metallic cobalt and cobalt(II) oxide. The end product under quasi-isothermal-isobaric conditions is metallic cobalt. Reactions (9) and (10) can proceed in parallel. A combination of (10) and the secondary reaction (11) cannot also be excluded:

$$CoO + CO \xrightarrow{exo} Co + CO_2 \quad (11)$$

It is assumed that the substages of stage II may be expressed by means of the reactions (12–14):

Substage IIa (air, argon)

Non-isothermal conditions

$$[Co(NH_3)_6]_2(C_2O_4)_3 \xrightarrow{endo} 3Co[Co(NH_3)_2(C_2O_4)_2] + N_2 + 28NH_3 + 3H_2O + 3CO + 3CO_2 \quad (12)$$

and reaction (5)

Quasi-isothermal-isobaric conditions

$$3[Co(NH_3)_{6-n}C_2O_4]_2(C_2O_4) \rightarrow 3Co[Co(NH_3)_2(C_2O_4)_2] + N_2 + (28\text{-}6n)NH_3 + 3H_2O + 3CO + 3CO_2 \quad (13)$$

Substage IIb (air, argon)

Non-isothermal, quasi-isothermal-isobaric conditions

$$3Co[Co(NH_3)_2(C_2O_4)_2] \xrightarrow{endo} 3Co[Co(C_2O_4)_2] + 6NH_3 \quad (14)$$

On the basis of some literature data, e.g. [8,38] it has been assumed that the agent reducing Co(III) to Co(II) is ammonia. Taking into account the investigation results of only the solid products of the decomposition this assumption cannot be proved explicitly. Also a hypothesis about oxalate ions as the reductor cannot be excluded as well. Then the overall reaction for the stage II would proceed according to the Eq. (15):

$$[Co(NH_3)_6]_2(C_2O_4)_3 \xrightarrow{endo} [Co[Co(C_2O_4)_2] + 12NH_3 + 2CO_2 \quad (15)$$

The verification of the assumed decomposition stages is possible only on the basis on the gas products investigation and is going to be a subject of our next article.

References

[1] E. Ingier-Stocka, A. Bogacz, J. Thermal Anal. 35 (1989) 1373.
[2] E. Ingier-Stocka, J. Thermal Anal. 37 (1991) 521, 769.
[3] E. Ingier-Stocka, Thermochim. Acta 170 (1990) 107.
[4] E. Ingier-Stocka, J. Thermal Anal. 50 (1997) 603.
[5] E. Ingier-Stocka, L. Rycerz, W. Szymański, A. Bogacz, in: Proc. XIX Oktobarsko Savetovnje Rudara, Metalurga i Technologa, Knjiga II, 147, Bor 1–2 oktobra, 1987 (in English).
[6] D. Dollimore, Thermochim. Acta 117 (1987) 331.
[7] A. Coetzee, D.J. Eve, M.E. Brown, J. Thermal Anal. 39 (1993) 947.
[8] W.W. Wendlandt, J.P. Smith, The Thermal Properties of Transition-Metal Amine Complexes, Elsevier, Amsterdam, 1967, pp. 37–103, 43.
[9] F. Paulik, Special Trends in Thermal Analysis, Wiley, Chichester, 1995, p. 384.
[10] W. Hadrich, Dissertation, Eberhard-Karls-Universitaet zu Tubingen, 1979.
[11] G.L. Jeyaraj, J.E. House Jr, Thermochim. Acta 68 (1983) 201.
[12] J. Bjerrum, J.P. McReynolds, Inorg. Synt. 2 (1946) 220.
[13] K. Nakamoto, Infrared and Raman Spectra of Inorganic and Coordination Compounds, 4rth Edition, Wiley, New York, 1986.

[14] R.A. Nyquist, R.O. Kagel, Infrared Spectra of Inorganic Compounds (3800–45 cm^{-1}), Academic Press, New York, 1971, No. 757.
[15] T.A. Dik, M.W. Nikanowicz, D.S. Umrejko, Koord. Khim. 15 (1989) 995.
[16] L. Sacconi, A. Sabatini, P. Gans, Inorg. Chem. 3 (1964) 1772.
[17] T. Shimanouchi, I. Nakagawa, Spectrochim. Acta 18 (1962) 89.
[18] K. Nagase, K. Sato, N. Tanaka, Bull. Chem. Soc. Japan 48 (1975) 868.
[19] K. Nagase, K. Sato, N. Tanaka, Bull. Chem. Soc. Japan 48 (1975) 439.
[20] K. Wieghardt, Z. Anorg. Allg. Chem. 391 (1972) 142.
[21] K.L. Scott, K. Wieghardt, A.G. Sykes, Inorg. Chem. 12 (1973) 655.
[22] S. Fronaeus, R. Larson, Acta Chem. Scand. 14 (1960) 6.
[23] Ch. J. Pouchert (Ed.), The Aldrich Library of Infrared Spectra, 3rd Edition, 1981.
[24] N.A. Czumajewskij, O.U. Szaropow, Zhurn. Neorg. Khim. 33 (1988) 1914.
[25] T.W. Swaddle, P.J. Craig, P.M. Boorman, Spectrochim. Acta 25A (1970) 1559.
[26] A. Grabowska, Master Thesis, Technical University of Wroclaw, 1996.
[27] A.B.P. Lever, Inorganic Electronic Spectroscopy, 2nd Edition, Elsevier, Amsterdam, 1984.
[28] V.S. Sastri, C.H. Langford, Can. J. Chem. 47 (1969) 4237.
[29] N. Deb, P.K. Gogoi, N.N. Dass, J. Thermal Anal. 35 (1989) 27.
[30] F.L. Urbach, R.D. Bereman, J.A. Topich, M. Hariharan, B.J. Kalbacher, J. Am. Chem. Soc. 96 (1974) 5063.
[31] P.W. Ball, A.B. Blake, J. Chem. Soc. A. (1969) 1415.
[32] B.N. Figgis, J. Lewis, Magnetochemistry in Technique of Inorganic Chemistry, Wiley, New York, 1965, p. 142.
[33] Landolt-Bornstein, E. Konig, Numerical data and functional relationships in science and technology, in: K.H. Hellwege (Ed.), Magnetic Properties of Coordination and Organo-Metallic Transition Metal Compounds, Springer, Berlin, 1966.
[34] Witte-Weiss, Magnetochemie, Weinheim, 1973, p. 155–166.
[35] L. Strinna Erre, G. Micera, B. Gulinati, F. Cariati, Polyhedron 11 (1992) 101.
[36] D.M.S. Mosha, D. Nicholls, Inorg. Chim. Acta 38 (1980) 127.
[37] JCPDS Mineral Powder Diffraction Data Files, International Centre for Diffraction Data, Park Lane, PA, USA.
[38] L.W. Collins, W.W. Wendlandt, Thermochim. Acta 8 (1974) 315.